Complementarity and Preorganization

James B. Wittenberg and Lyle Isaacs
University of Maryland, College Park, MD, USA

1 INTRODUCTION

The pioneering work of Pedersen, Lehn, and Cram in the area of cation recognition laid the groundwork on which much of contemporary supramolecular chemistry is based.[1–4] For example, would the ensembles that function as chemosensors for ions and molecules be conceivable without receptors that bind strongly and selectively toward their targets?[5,6] Could supramolecular systems that respond to external stimuli—molecular machines—be designed without an intricate knowledge of the binding free energies between different stations before and after the stimulus?[7,8] Imagine the state of the art in drug discovery without a fundamental understanding of the principles that govern the formation of compounds and complexes that are shaped and held together by noncovalent interactions.[9,10] In this chapter, we discuss two fundamental concepts—the principles of complementarity and preorganization—that have been widely used in the design of new host–guest systems.

Supramolecular Chemistry: From Molecules to Nanomaterials.
Edited by Philip A. Gale and Jonathan W. Steed.
 ISBN: 978-0-470-74640-0.

2 DISCUSSION

This discussion section first presents the concepts of complementarity and preorganization from a conceptual point of view. Subsequently, each of these concepts is elaborated upon in a tutorial fashion by the presentation of a series of classical and contemporary examples from the literature. Finally, we introduce some related concepts that arise from current research in supramolecular chemistry.

2.1 Concepts of complementarity and preorganization

The interaction between host and guest is driven by the same fundamental noncovalent interactions (e.g., hydrogen bonding, $\pi-\pi$ interactions, electrostatic interactions, and van der Waals interactions) that dictate the interaction between solvent molecules and hosts and solvent molecules and guests. Given the generally much higher concentration of solvent relative to host and guest, effective host–guest complexation requires that numerous weak noncovalent interactions between host and guest act in concert to outcompete solvent molecules (e.g., solvation). Cram's statement of the *principle of complementarity* is as follows: "to complex, hosts must have binding sites which can simultaneously contact and attract the binding sites of the guests without generating internal strains or strong nonbonded repulsions."[1] In this manner, the complementarity between host and guest is the major factor governing mutual recognition between molecules. Although complementarity is necessary for structural recognition between molecules, it is in many cases not sufficient to drive complex formation. Consider two hosts, both of which possess a single conformation that is complementary to a specific guest but differ in their conformational properties. One host is rigid and can

only adopt a single low-energy conformation, whereas the second host is flexible and can adopt numerous conformations. In order to form a host–guest complex, the flexible host must overcome the energetic (entropic and enthalpic) costs associated with restricting itself to a single conformation which reduces the overall binding free energy. Cram refers to this concept as the *principle of preorganization* and defines it as follows: "the more highly hosts and guests are organized for binding and low solvation prior to their complexation, the more stable will be their complexes."[1]

2.2 Types of complementarity

This section presents examples of complementarity in host–guest systems organized by the type of noncovalent interaction involved in the recognition process.

2.2.1 *Lock-and-key versus induced fit*

In 1894, Emil Fischer formulated the lock-and-key model of enzyme action.[11] The lock-and-key model holds that the active site of the enzyme is rather rigid and that the enzymatic substrate must possess an exactly complementary shape (Figure 1), which explains the high levels of specificity exhibited by enzymes. In the terminology of supramolecular chemistry, an enzyme that follows the lock-and-key model would obey both the *principle of complementarity* and the *principle of preorganization* with the exception that an enzyme active site may be solvated before binding. As we have seen above, many synthetic host–guest systems are not fully preorganized and may require conformational changes or change of tautomeric state in order to become most complementary to the guest at hand and this endows these systems with a level of environmental responsiveness. The observation of this type of behavior in supramolecular systems has ample precedents in biochemistry. For example, Koshland formulated the induced fit theory that holds that "the substrate may cause an appreciable change in the three-dimensional relationship of the amino acids at the active site" (Figure 1).[12] Just as biochemistry progressed beyond a simple lock-and-key theory to include concepts of induced fit complementarity toward diverse substrates, so does contemporary supramolecular chemistry with the development of nonpreorganized systems that are stimuli responsive.

2.2.2 *Hydrogen bonds*

Perhaps, the best studied class of noncovalent interaction is the hydrogen bond.[13–20] Hydrogen bonds are formed between electrostatically negative atoms—most commonly heteroatoms like oxygen and nitrogen that bear lone

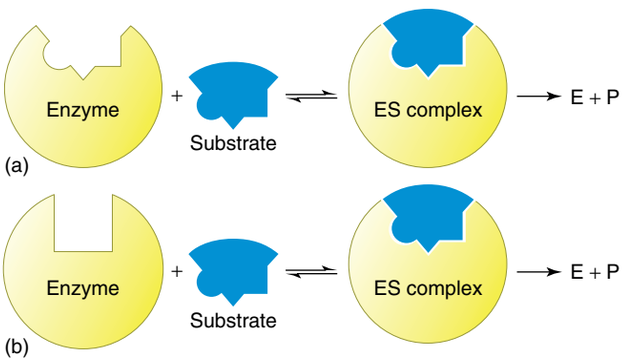

Figure 1 (a) Interaction of enzyme with substrate by a lock-and-key mechanism to give the enzyme–substrate complex. (b) Interaction of enzyme with substrate by an induced fit mechanism to give the enzyme–substrate complex.

pairs—that act as hydrogen bond accepting (A) groups and electrostatically positive acidic hydrogen atoms also generally bonded to heteroatoms like oxygen and nitrogen that act as hydrogen bond donating (D) groups. The hydrogen bond is best thought of, to a first approximation, as an electrostatic interaction between two dipoles. For example, Figure 2 illustrates two geometries for the interaction between **1** and **2** which contain C=O acceptor and N–H donor groups and also for **3** which contains RO acceptor and O–H donor groups. In both cases, the negative end of the acceptor dipole (e.g., C=O or O) interacts with the positive end of the donor dipole (e.g., O–H or N–H). Studies of the Cambridge Structural Database (CSD) reveal a preference for a linear or near-linear arrangement of the O···H–N atoms involved, which is present in both Geometry A and Geometry B.[13] Taylor and Kennard also report that "there is a distinct preference for N–H···O=C hydrogen bonds to form in, or near to, the directions of the sp^2 lone pairs."[13] Figure 2(d) shows that the shorter and stronger H-bonds have NH···O angles close to 180°, whereas H-bonds with smaller NH···O angles are longer and weaker.[13] Accordingly, molecules that interact by way of a single H-bond donor and a single H-bond acceptor that satisfy these geometrical requirements are complementary to one another. When pairs of molecules interact by the formation of two or more hydrogen bonds, one must consider the overall complementarity between molecules that leads to the energetically most stable geometry. For example, carboxylic acid groups generally form cyclic dimers (**4·4**), whereas ureas commonly form chains that adopt the basic interaction motif (**5·5**) shown in Figure 2. In the sections below, we discuss in more detail complementarity in systems driven by the formation of multiple hydrogen bonds.

The importance of the hydrogen bond in determining the structure and function of Nature's biomolecules (e.g., DNA, RNA, proteins) is well known.[21] We, therefore, restrict our

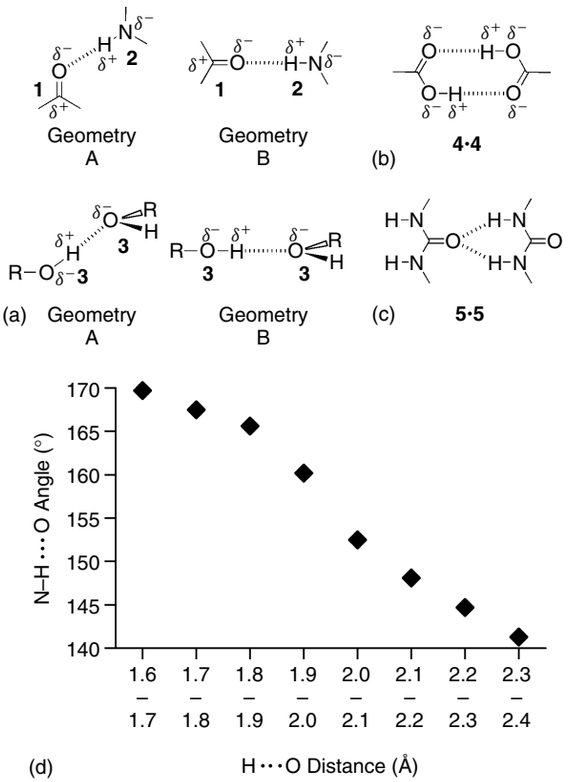

Figure 2 (a) Line bond drawing of two different geometries (A and B) for NH···O and OH···O H-bonded species, (b) H-bond pattern for the acetic acid dimer **4·4**, (c) typical H-bond pattern for the interaction between two ureas **5·5**, and (d) H···O bond distance as a function of NH···O angle.

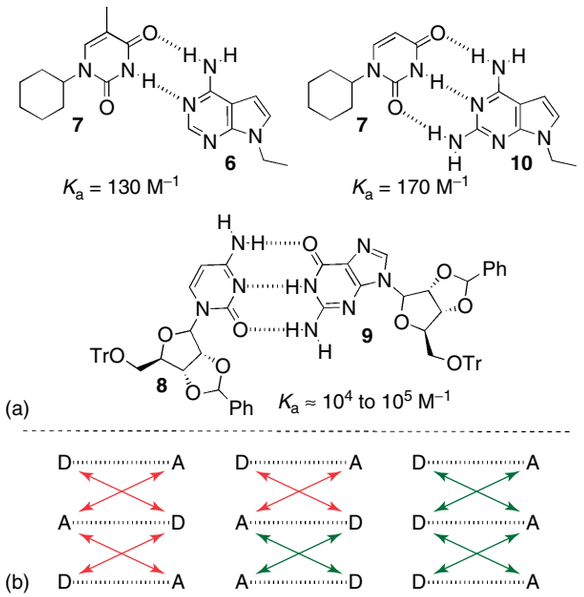

Figure 3 (a) Chemical structures and association constants for H-bonding pairs **7.6, 7.10**, and **8.9**, and (b) representation of the primary H-bonds (black dashed lines) and secondary H-bonding interactions (green arrows, favorable secondary interactions; red arrows, unfavorable secondary interactions) for three different triply H-bonded pairs.

discussion to those aspects of H-bond-driven association that are relevant for complementarity and preorganization. Within the context of DNA hybridization, the nucleobases adenine (A) and thymine (T) or cytosine (C) and guanine (G) undergo association driven by the formation of two or three H-bonds, respectively. Rich and coworkers studied the association between 9-ethyladenine (**6**) and 1-cyclohexylthymine (**7**) in $CDCl_3$ solution by infrared spectroscopy and determined $K_a = 130\,M^{-1}$ (Figure 3).[22] The **6·7** complex is driven by the formation of two H-bonds. In contrast, the complex between cytidine derivative (**8**) and guanosine derivative (**9**) in $CDCl_3$ is driven by the formation of three hydrogen bonds with $K_a \approx 10^4$ to $10^5\,M^{-1}$.[23] As might be naively expected, the addition of a third H-bond enhances the overall driving force of the complexation significantly. However, not all complexes held together by three H-bonds are so stable. For example, the complex between **7** and **10** has $K_a = 170\,M^{-1}$ in chloroform solution.[22] What is the major factor responsible for the dramatic difference in affinity between the **8·9** and **7·10** complexes that are both driven by the formation of three H-bonds? This question was addressed in a classic paper by Jorgensen and Pranata by computational methods.[24] Jorgensen and Pranata suggest that the origin of these differences are due to secondary electrostatic interactions. Complex **7·10** is formed from the complementary DAD and ADA H-bonding arrays of **7** and **10**, respectively, whereas the **8·9** complex is formed from the complementary DAA and AAD H-bonding arrays of **8** and **9**, respectively. In addition to the three H-bonds (black dashed lines) between the partners, the DAD–ADA complex has four unfavorable secondary electrostatic interactions (red arrows), whereas the DAA–AAD complex possesses two unfavorable and two favorable (green arrows) electrostatic interactions (Figure 3b). Analysis of a hypothetical complex held together by the DDD–AAA H-bonding array reveals the presence of four favorable secondary interactions. Jorgensen and Pranata conclude that consideration of secondary electrostatic effects "have general applicability in hydrogen-bonding complexation in many contexts."[24]

Shortly after the reports of Jorgensen, the Zimmerman group published the first example of the DDD–AAA H-bonding pair **11·12** (Figure 4). The value of K_a exceeded the limit of K_a values accessible by ^{1}H NMR (nuclear magnetic resonance) titrations; accordingly they report a lower limit of $K_a > 10^5\,M^{-1}$.[25] Subsequently, Anslyn and Bell reported a cationic DDD–AAA H-bonding pair **13·12** and attempted to determine its K_a value by

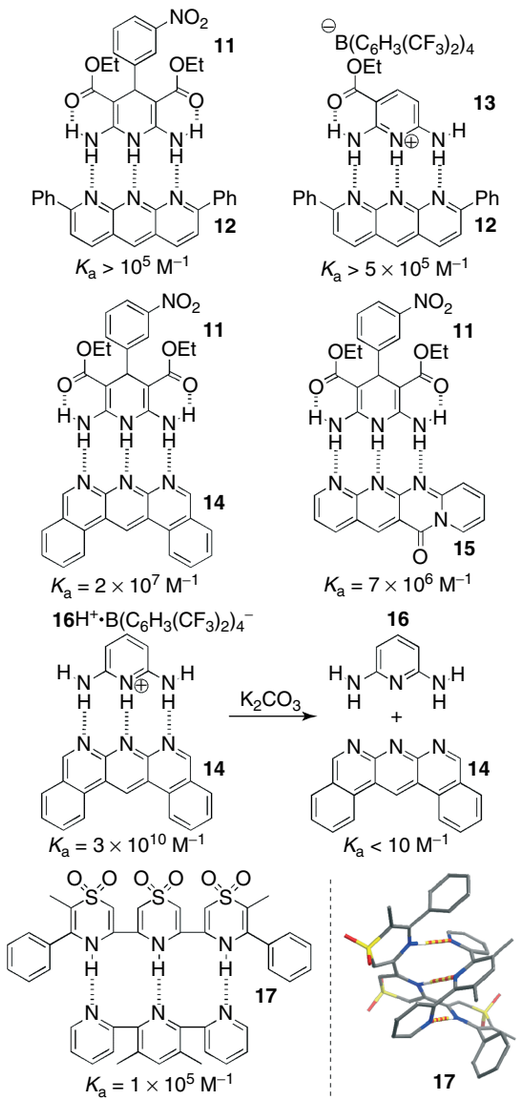

Figure 4 Chemical structures of DDD–AAA triply H-bonded pairs **11·12, 12·13, 11·14, 11·15, 14·16**H$^+$, and **17** studied by the Zimmerman, Anslyn, Leigh, and Wisner groups.

UV–vis spectroscopic methods.[26] Once again, the K_a value exceeded the range that was accessible by UV–vis measurements and only a lower limit of $K_a > 5 \times 10^5\,M^{-1}$ could be given. Very recently, the Wisner group reported a stable double helical complex through an AAA–DDD array and determined the K_a value for **17** ($K_a = 1 \times 10^5\,M^{-1}$) in $CDCl_3$ by ^{1}H NMR.[27] Also recently, the Leigh group synthesized **14** and **15** which features a DDD array and which is also highly fluorescent. Accordingly, the Leigh group used fluorescence spectroscopy as the analytical technique—which greatly expands the range of K_a values that are accessible—to determine the K_a values for the **11·14** ($K_a = 2 \times 10^7\,M^{-1}$), **11·15** ($K_a = 7 \times 10^6\,M^{-1}$), and **14·16**H$^+$ ($K_a = 3 \times 10^{10}\,M^{-1}$) complexes. Clearly, secondary electrostatic interactions can play a dramatic role in determining the overall affinity of H-bonded complexes. Leigh and coworkers conclude that "in this series each incremental increase of two cooperative secondary interactions increases the stability of the neutral triple hydrogen bonded complex by roughly 3 kcal mol^{-1}."[28] Addition of solid K_2CO_3 to **14·16**H$^+$ deprotonates **16**H$^+$ to give **16** which has a DAD H-bonding array. Proton NMR titration experiments between **14** and **16** in CD_2Cl_2 at millimolar concentrations do not reveal any interactions between **14** and **16** ($K_a > 10\,M^{-1}$). The introduction of a single noncomplementary H-bonding interaction reduces binding affinity by 10^9-fold! Such stimuli-induced changes in K_a and the corresponding changes in ΔG provide a potent driving force for the current generation of molecular machines.[7]

Given the analysis described above, which shows that the value of K_a for hydrogen-bonded assemblies increases as the number of hydrogen bonds increases, it is perhaps not surprising that a number of investigators have constructed assemblies driven by a multitude of hydrogen bonds. One example comes from the work of Ghadiri, who prepared **18** (Figure 5).[29] Compound **18** is a cyclic decapeptide composed of alternating hydrophobic D- and L-amino acids, and adopts a circular structure with H-bond donors and acceptors oriented perpendicular to the plane of the macrocycle. Accordingly, **18** undergoes H-bond-mediated assembly to form nanotubular assemblies. Addition of **18** to an aqueous solution of phosphatidylcholine liposomes results in their assembly in the membrane into channels of ≈10 Å diameter. In a related experiment, the addition of **18** to a solution of glucose-entrapped unilamellar lipid vesicles results in efflux of glucose as monitored by the absorbance of NADPH (nicotinamide adenine dinucleotide phosphate-oxidase) at 340 nm produced in an enzyme-coupled assay.[29]

A particularly interesting example of association driven by the formation of four H-bonds that features issues of complementarity and preorganization was reported by Zimmerman.[30] Corbin and Zimmerman synthesized ureidodeazapterin **19** which—unlike the H-bonding systems described above—has the potential for prototropic equilibria (Figure 6). Compound **19** presents an AADD-H-bonding array which is self-complementary and therefore undergoes dimerization to yield **19·19** in $C_6D_5CD_3$ and $CDCl_3$. However, **19** can undergo prototropy to yield **20**–**23** which present AADD-, ADAD-, ADDA-, and ADDA-H-bonding arrays, respectively. Protomers **20** and **21** are, of course, also self-complementary and form homodimers **20·20** and **21·21**. Because **19** and **20** both possess AADD-H-bonding arrays, they are also complementary to each other and are capable of forming the heterodimer **19·20**. In total, three homodimers and one heterodimer are observed in $C_6D_5CD_3$

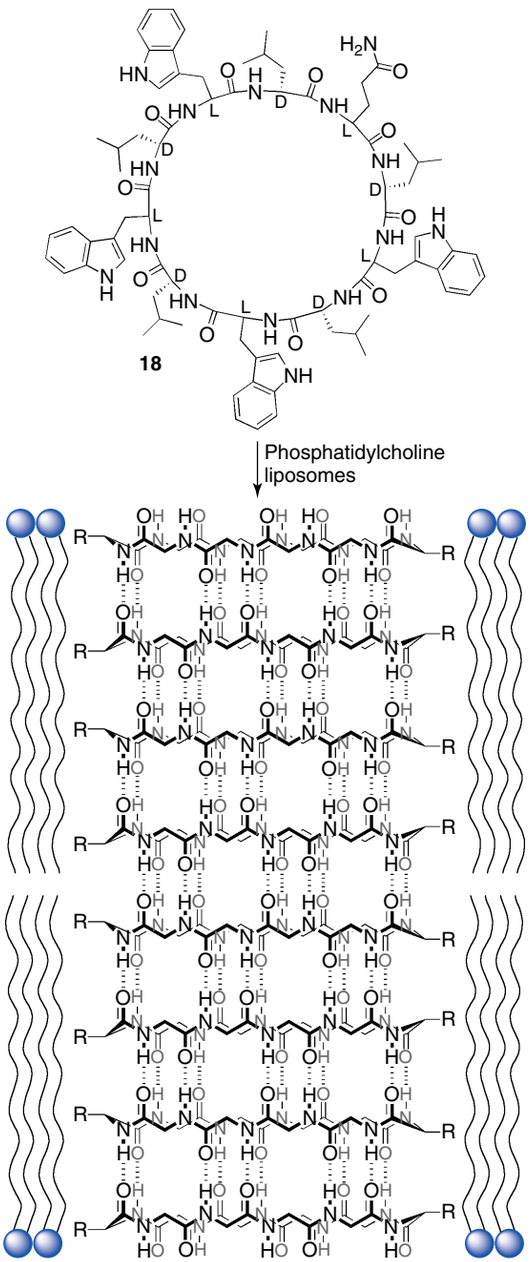

Figure 5 Chemical structure of Ghadiri's cyclic peptide **18** which undergoes self-association in phosphatidylcholine liposomes to form nanotubes that transport glucose across the membrane.

to the exclusion of monomer as a result of the high K_a value ($K_a > 10^7\ M^{-1}$) for this quadruply H-bonded DDAA-based system. Interestingly, protomers **22** and **23** feature ADDA-H-bonding arrays that are not self-complementary and not observed in $C_6D_5CD_3$ solution. Addition of diamidonaphthyridine **24**, which features a DAAD-H-bonding array that is complementary to the ADDA-H-bonding array of protomers **22** and **23**, dramatically alters the prototropic equilibrium with the exclusive formation of a mixture of the **22·24** and **23·24** heterodimers. In this way, **22** and **23** can be viewed as being complementary to **24** but are not preorganized for heterodimerization because of the energetic costs associated with breaking up dimers **19·19**–**21·21** and **19·20** as well as tautomerization to **22** and **23**. Complementarity is a complex property because most molecules exist in a variety of conformations and some even possess prototropic forms each of which possesses a specific complementarity. Beyond this, some compounds possess two or more potentially overlapping binding locations[31] which can further complicate the situation.

2.2.3 Electrostatic interactions

Electrostatic effects can play a very large role in determining the overall strength and geometry of noncovalent complexes. Most generally, positively charged regions of molecules are attracted to negatively charged regions of their partners. In supramolecular systems, such interactions most commonly take the form of ion–ion, ion–dipole, ion–quadrupole, and quadrupole–quadrupole interactions. Of course, the strength of such interactions falls off as one proceeds from ion to dipole to quadrupole.[32]

Ion–dipole interactions

The pioneering work of Pedersen on the crown ethers constitutes the premiere example of ion–dipole interactions in supramolecular chemistry.[2] Figure 7 shows idealized chemical structures of 12-crown-4, 15-crown-5, and 18-crown-6, which are prototypical members of the crown ether series of macrocycles discovered by Pedersen.[33] By a combination of methods, most notably solubility measurements and UV spectroscopy, Pedersen showed that the crown ethers form complexes with a variety of alkali-metal cations (e.g., Li^+, Na^+, K^+, Cs^+) and also with ammonium ions mainly in CH_3OH as solvent. Figure 7 shows a representation of the geometry observed in the X-ray crystal structure of 18-crown-6 subsequently determined by Dunitz and Trueblood,[34] which shows that two of the CH_2 groups turn inward and fill the cavity of the receptor. In the presence of KSCN (potassium thiocyanate), 18-crown-6 undergoes a conformational change that results in the formation of the 18-crown-6·K^+ complex depicted in Figure 7. In this manner, 18-crown-6 is complementary toward K^+ ion but is not preorganized for binding. The driving force for the formation of the 18-crown-6·K^+ complex is ion–dipole interactions between the K^+ ion and the dipole associated with the ether O atoms. Through the combined efforts of a large number of researchers, the structural features (e.g., number of coordinating atoms, identity of coordinating atoms, types and geometry of

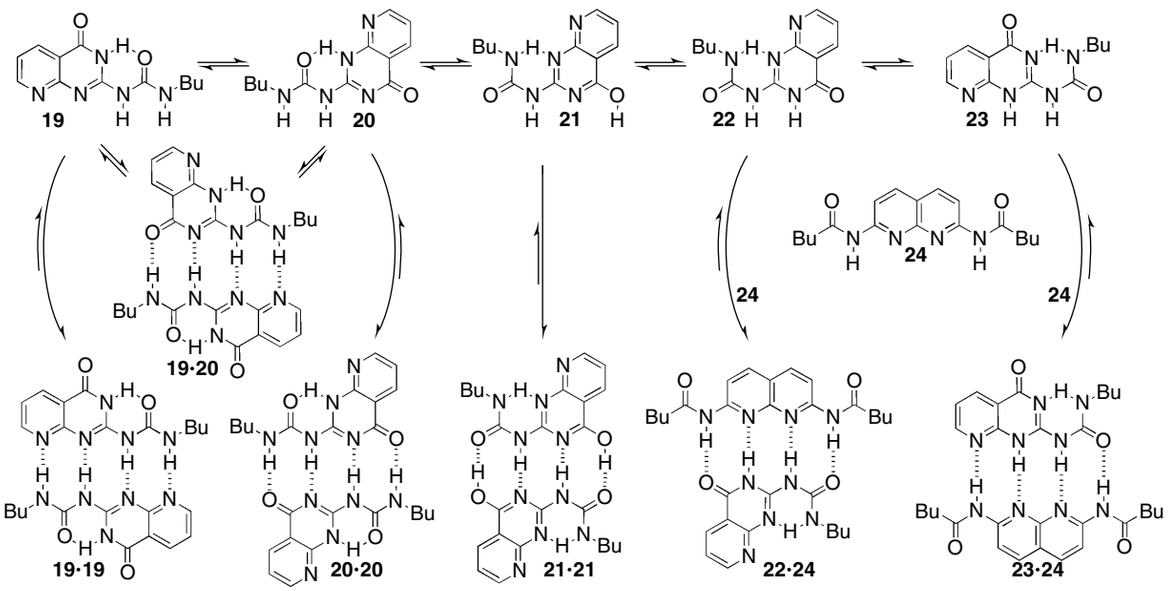

Figure 6 Chemical structures of tautomeric forms of monomeric ureidodeazapterin (**19**–**23**), homodimers (**19·19, 20·20**, and **21·21**), and heterodimers (**19·20, 22·24, 23·24**).

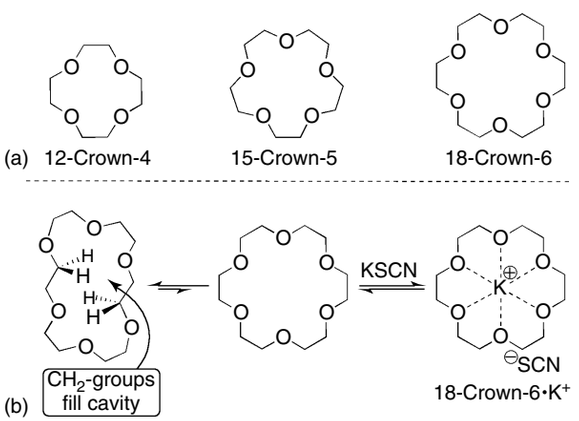

Figure 7 (a) Chemical structures of 12-crown-4, 15-crown-5, and 18-crown-6, and (b) illustration of the conformational change that occurs upon binding of K^+ ion.

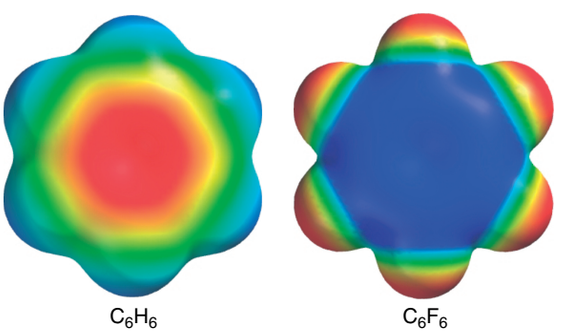

Figure 8 Electrostatic potential surfaces for benzene and hexafluorobenzene spanning the range from −60 (red) to +50 (blue) kcal mol^{-1}.

bridges) toward the complexation of cations have been delineated. For the purpose of this discussion, one of the most interesting features of the complexation behavior of crown ethers is their selectivity toward alkali cations based on size. For example, among the series of alkali cations (M^+, ΔG kcal mol^{-1}; Na^+, −5.89; K^+, −8.27; Rb^+, −7.26; Cs^+, −6.06)[35] 18-crown-6 displays highest affinity toward K^+ in CH_3OH because the size of this cation matches best to the size of the cavity.

Interactions with quadrupoles

Molecules that are centrosymmetric (e.g., benzene) do not possess a molecular dipole moment. The distribution of electrons within a benzene molecule, however, is not symmetrical, with the region above the plane of the aromatic ring constituting a region of negative electrostatic potential and the H-atoms around the aromatic ring constituting a region of positive electrostatic potential (Figure 8). For this reason, benzene has a nonzero quadrupole moment and is capable of noncovalent interactions of, for example, the ion–quadrupole and quadrupole–quadrupole type.

The research group of Dougherty[36,37] extensively studied the binding properties of anionic cyclophane **25** (Figure 9). They found that **25** displays high affinity toward cationic species in water. For example, *N*-methylquinolinium **26** and *N*-methylisoquinolinium **27** bind to **25** with ΔG° values of −8.4 and −7.3 kcal mol^{-1}, respectively, at pH 9.0 in 10 mM borate-buffered water. In contrast, **25** binds far more weakly with quinoline **28** ($\Delta G^\circ = -5.3$ kcal mol^{-1})

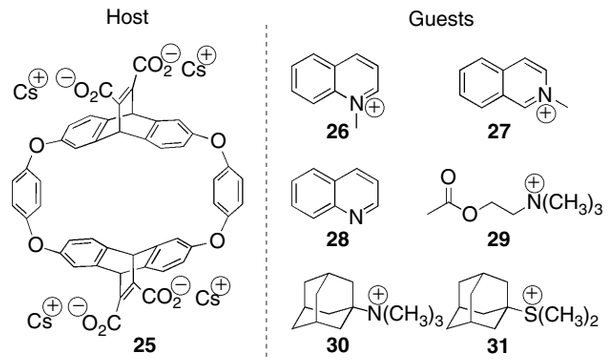

Figure 9 Chemical structure of cyclophane **25** and some of its guests (**26**–**31**).

which is neutral in borate buffer. Tight binding is not restricted to aromatic ammonium ions, but is also possible with aliphatic ammonium ions. For example, acetylcholine (**29**) and 1-trimethylammonium adamantane (**30**) are very good guests ($\Delta G^\circ = -6.2$ and $-6.7\,\text{kcal mol}^{-1}$) for **25**. Intriguingly, sulfonium cations are also excellent guests for **25**, and **31** which is the *S*-analog of **30** binds nicely ($\Delta G^\circ = -5.7\,\text{kcal mol}^{-1}$). The patterns of ^{1}H NMR chemical shifts for **25.30** and **25.31** are similar, which suggests that these complexes adopt a common geometry. The results discussed here, along with numerous other host–guest complexes discussed by Dougherty as well as theoretical calculations, establish that these complexes benefit from a cation–π interaction that is predominantly electrostatic (e.g., ion–quadrupole) in origin.

Similar to benzene, hexafluorobenzene possesses no molecular dipole moment because it is centrosymmetric. As a result of the high electronegatively of F atoms, however, the fluorinated rim of C_6F_6 constitutes a region of high negative electrostatic potential, and the regions above and below the plane of the aromatic rings are in fact electrostatically positive (Figure 8). Benzene and hexafluorobenzene have sizable molecular quadrupole moments of similar magnitude but of opposite sign.[38] Interestingly, C_6H_6 (m.p. 5.5 °C) and hexafluorobenzene (m.p. 4 °C) form a 1 : 1 cocrystal (m.p. 24 °C) which consists of stacks of alternating molecules. A very interesting example of a quadrupole–quadrupole interaction was utilized by Dougherty *et al.*[39] to promote polymerization of diynes in the solid state. They synthesized **32**–**34** and obtained 1 : 1 cocrystals of **32** and **33** as well as crystals of **34** (Figure 10). As expected, the cocrystals of **32** and **33** adopt an alternating stacking geometry in the crystal which brings the diyne units in close proximity (center-to-center distance ≈3.7 Å; $\Phi \approx 75^\circ$). Photolysis of the crystals or powdered samples resulted in the alternating copolymerization of **32** and **33** as confirmed by fast-atom bombardment mass spectrometry.

2.2.4 *Size and shape*

Complementarity between the size and shape of a guest and the size and shape of the cavity of its cognate host is of critical importance in determining the binding strength. When the molecular surfaces of the host and guest are able to embrace but not overlap, the noncovalent interaction between them will be maximized. Excellent examples of the importance of size and shape complementarity in host–guest complexation are available with the cucurbit[*n*]uril (CB[*n*]) family of macrocycles (see **Cucurbituril Receptors and Drug Delivery**, Volume 3).[40,41] CB[*n*] compounds ($n = 5$, 6, 7, 8, 10) are readily prepared by the condensation of glycoluril (1 equivalent) with formaldehyde (2 equivalent) in hot (e.g., <100 °C) concentrated HCl in high overall yield (Figure 11). The defining features of the CB[*n*] family of macrocycles are the presence of a hydrophobic cavity guarded by two symmetrically equivalent portals of high negative electrostatic potential. Because CB[*n*] compounds are built from fused five- and eight-membered rings, they are rather rigid and preorganized and therefore exhibit high binding constants toward suitable cationic guest molecules. A prototypical guest for the CB[6] molecular container

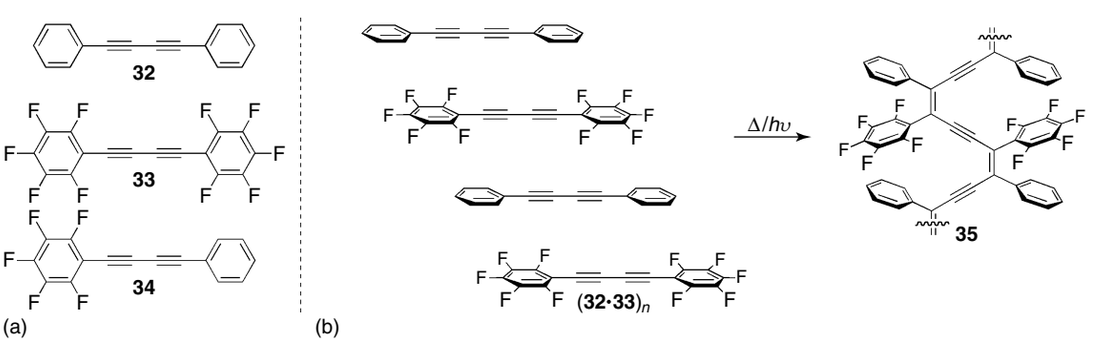

Figure 10 (a) Chemical structures of diynes **32**–**34** and (b) illustration of the packing of **32** and **33** in a 1 : 1 cocrystal and its transformation into polydiacetylene **35**.

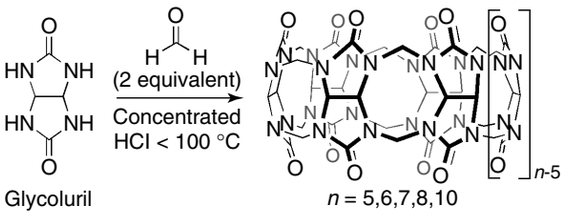

Figure 11 Synthesis of CB[*n*].

is hexanediammonium ion (**36**) which binds with $K_a = 4.5 \times 10^8\ M^{-1}$ (50 mM acetate-buffered D_2O, pH 4.74) due to a combination of the hydrophobic effect, H-bonding, and ion–dipole interactions (Figure 12).[42] For example, CB[6] readily binds to cyclopentylmethylammonium **37** ($K_a = 330\,000\ M^{-1}$), which has a cavity volume of 86 Å^3 but binds 1000-fold more weakly to *p*-$CH_3C_6H_4CH_2NH_3^+$ **38** (320 M^{-1}) which has a volume of 89 Å^3.[43] In a related manner, CB[6] binds to *p*-methylanilinium ion (**39**) nicely ($K_a = 1265\ M^{-1}$) but completely rejects the *m*- and *o*- isomers (**40a** and **b**). Similar phenomena have been observed in the binding of the larger CB[*n*] homologs CB[7] and CB[8] whose cavity volumes of 272 and 474 Å^3 parallel those of β- and γ-cyclodextrin. For example, CB[7] binds with remarkable affinity to adamantaneammonium ion **41** ($K_a = 4.2 \pm 1.0 \times 10^{12}\ M^{-1}$) in 50 mM acetate-buffered D_2O at pH 4.74. The value of K_a for the CB[8]·**41** complex ($K_a = 8.2 \pm 1.8 \times 10^8\ M^{-1}$) is over 5000-fold lower! Apparently, there is an outstanding match between the size and shape of the adamantane residue and the cavity of CB[7]. In contrast, the addition of two CH_3 groups renders the CB[7]·**42** complex ($K_a = 2.5 \pm 0.4 \times 10^4\ M^{-1}$) over 10^8-fold weaker than the corresponding CB[7]·**41** complex. The addition of these two CH_3 groups results in energetically costly interactions between the CH_3 groups and the walls of the CB[7] host. Overall, the CB[*n*] family of molecular containers constitute one of the most selective purely synthetic host platforms known with affinities that rival and in some cases exceed those of the natural counterparts (e.g., protein–ligand or antibody–antigen interactions).[31]

2.2.5 *Van der Waals interactions*

Compared to H-bonds or ion–dipole interactions, van der Waals interactions are relatively weak, and large surface areas must come into contact for stable complexes to result. A particularly elegant example of dimerization driven by van der Waals interactions comes from the work of Cram and Cram.[1] For example, Cram and coworkers prepared compounds **43a–c** which all feature a resorcinarene bowl functionalized with four quinoxaline rings and differ in the nature of the substituent (H, CH_3, Et) attached to the rim (Figure 13).[44] Compound **43** has the potential to exist in at least two main conformations, which Cram refers to as the "vase" and the "kite" conformation. Examination of CPK (creatine phosphokinase) models suggests that the vase conformation is strain-free, whereas the kite conformation is strained. Quite interestingly, variable temperature NMR measurements indicate that the C_{4v}-symmetric vase **43a** is preferred above 45 °C and the C_{2v}-symmetric kite **43a** conformation is preferred below −62 °C in $CDCl_3/CS_2$ (1 : 1). Apparently, the larger solvent-exposed surface of kite **43a** results in an enthalpically favorable solvation of kite **43a** relative to vase **43a,** which outweighs the unfavorable entropic contributions of solvation toward this equilibrium at low temperatures. In contrast, compounds **43b** and

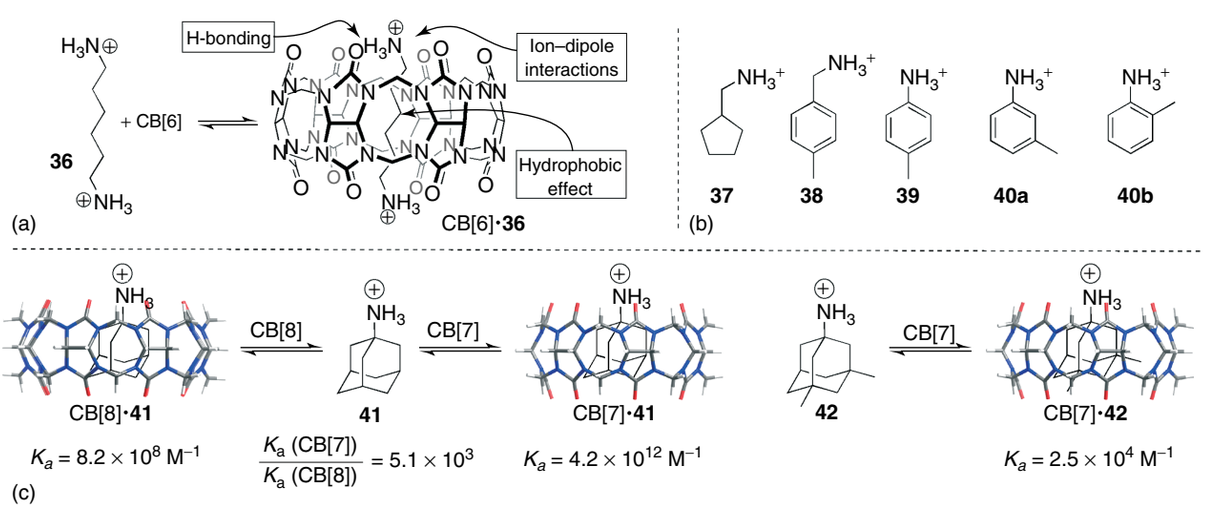

Figure 12 (a) Illustration of the noncovalent interactions driving the formation of CB[6]·**36**, (b) structure of guest compounds **37–40**, and (c) illustration of high levels of selectivity in the recognition behavior of CB[*n*] compounds.

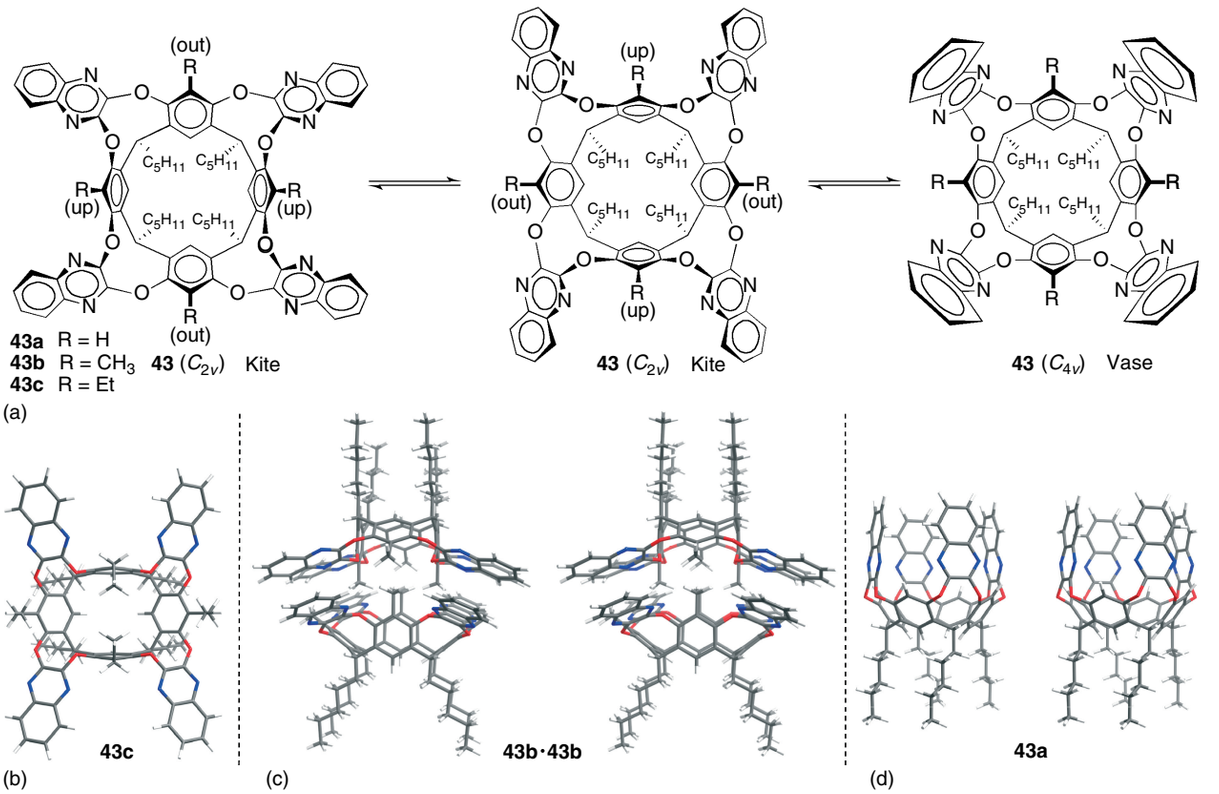

Figure 13 (a) Conformational behavior of **43**, and Merck Molecular Force Field (MMFF)-minimized geometries of (b) **43c**, (c) cross-eyed stereoview of **43b·43b**, and (d) cross-eyed stereoview of **43c**.

43c are found to exist in the kite conformation exclusively. Cram attributes this preference to the presence of severe steric interactions between the lone pairs on the quinoxaline N atoms and the adjacent CH_3 or Et groups in the hypothetic vase conformer. The CH_3 and Et groups override the innate conformational preferences and preorganize **43b** and **43c** into the kite conformation which features a largely aromatic surface of roughly 15×20 Å dimension. Compound **43b** undergoes monomer–dimer equilibrium in $CDCl_3$ ($\Delta G^\circ = -6.8\,\text{kcal mol}^{-1}$) as evidenced by a variety of analytical techniques including vapor pressure osmometry, ^{1}H NMR spectroscopy, X-ray crystallography, and mass spectrometry. This remarkable dimeric structure **43b·43b** (Figure 13) features van der Waals interactions between the stacking quinoxaline rings and a critical complexation of the CH_3 groups of 1 equivalent of **43b** into the space on the opposing equivalent of **43b** shaped by the resorcinol-derived aromatic ring and four adjacent ether oxygen and vice versa. The 2 equivalents of **43b** are preorganized and fit together in a lock-and-key fashion. In contrast, the Et groups of **43c** are too large and inhibit dimerization. Compound **43c** exists as a monomer in solution and the solid state as evidenced by ^{1}H NMR and X-ray crystallography, respectively. A detailed analysis of the X-ray crystal structure of **43b·43b** reveals a total of 132 close contacts between molecules. This amounts to $0.052\,\text{kcal mol}^{-1}$ per close contact in $CDCl_3$ solution. Interactions between nonpolar surfaces in aqueous solution have been estimated to be worth $0.02–0.06\,\text{kcal mol}^{-1}$ Å^{-2}.[45]

2.2.6 *Spatial complementarity*

The level of complementarity between molecules is determined by the combination of the noncovalent interactions described above. In host–guest systems derived from achiral host or achiral guest, the corresponding host–guest complex will be either achiral or a racemic mixture. In contrast, if an enantiomerically pure host is combined with a chiral but racemic guest, two diastereomeric complexes are possible and one would expect to observe enantioselectivity in the complexation process. Nature's enantiomerically pure biomolecules display high levels of enantioselectivity in their interactions with their targets. This is one of the reasons why many of new pharmaceutical agents are prepared in enantiomerically pure rather than racemic forms. As such, studies of chiral recognition in designed systems are of tremendous academic and practical

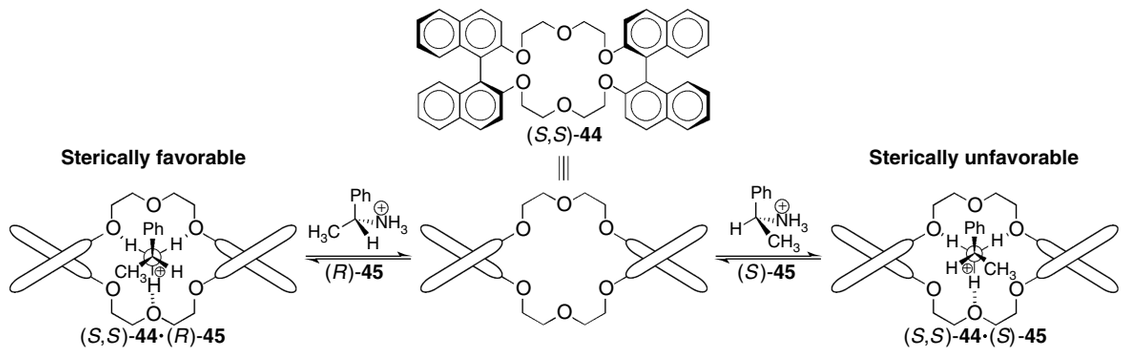

Figure 14 Chiral recognition of ammonium salt **45** by enantiomerically pure host (*S*,*S*)-**44**.

interest. An interesting early example of chiral recognition in designed supramolecular systems comes from the work of Cram.[46] Cram and coworkers developed enantiomerically pure cyclophane (*S*,*S*)-**44** based on binaphthol building blocks (Figure 14). It was found that (*S*,*S*)-**44** was able to selectively complex and extract (*R*)-**45** in preference to (*S*)-**45** from water into $CHCl_3$ as its PF_6^- salt. The extent of chiral recognition was modest (0.266 kcal mol^{-1}) but a number of aspects of this study are noteworthy. First, the enantiomeric preference was predictable. Figure 14 shows Newman-type projections of the (*S*,*S*)-**44**•(*R*)-**45** and (*S*,*S*)-**44**•(*S*)-**45** complexes. In the favored (*S*,*S*)-**44**•(*R*)-**45** complex, the CH_3 group of **45** is oriented roughly parallel to one of the naphthol walls, whereas in the (*S*,*S*)-**44**•(*S*)-**45** complex the same CH_3 group is oriented roughly perpendicular to the naphthol wall and develops an unfavorable steric interaction. Second, Cram and coworkers designed (*S*,*S*)-**44** such that it has overall C_{2v} symmetry and, therefore, complexation on either face of (*S*,*S*)-**44** produces an identical complex. Such symmetry considerations are now commonly employed in the development of chiral and enantiomerically pure catalysts for organic transformations. Lastly, Cram and coworkers used an analog **46** to prepare a machine that resolves amino esters by simultaneous complexation and transport of both enantiomers of the amino acid from a source aqueous phase through a membrane-like $CHCl_3$ phase and into a receiving aqueous phase (Figure 15).[1,47] Noteworthy aspects of this early work from a contemporary viewpoint were the use of a concentration gradient between the central and peripheral aqueous phases which acts as the thermodynamic driving force for the operation of the machine and the simultaneous use of both enantiomers of the host to drive the separation process more efficiently than if only one enantiomer were used. Such concepts are routinely encountered in contemporary supramolecular chemistry in the areas of membrane transport, stimuli-responsive molecular machines, and systems chemistry.[7,8,48–50]

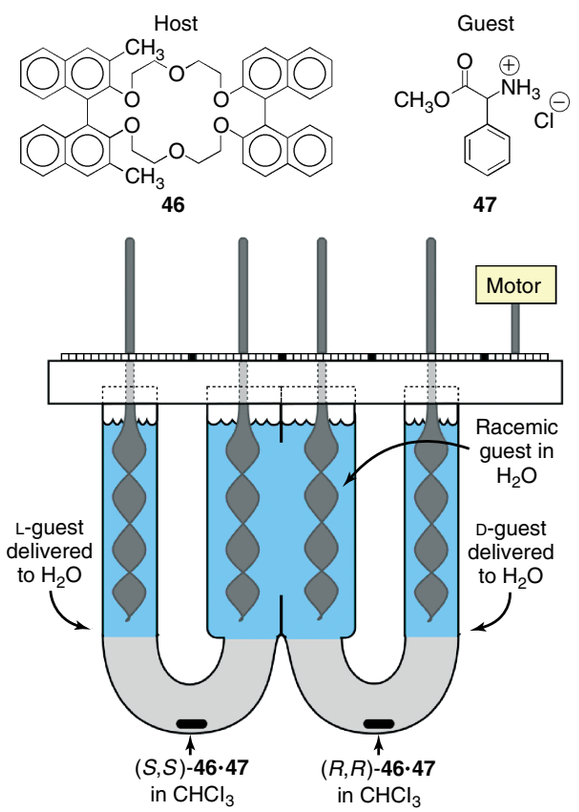

Figure 15 The amino ester resolving machine.

2.3 Types of preorganization

This section discusses some classical and contemporary examples of structural preorganization based either on the formation of macrocyclic hosts or on the use of acyclic hosts comprising multiple small rings fused together. Subsequently, we discuss the importance of desolvation on the degree of preorganization of the host which impacts the overall affinity of host toward guest.

2.3.1 Macrocyclic preorganization

Cram appreciated that the need for 18-crown-6 to undergo conformational changes (Figure 7) and desolvation (e.g., CH_3OH) would detract from the affinity of 18-crown-6 toward K^+ ions. Accordingly, Cram designed, synthesized, and studied a class of polyether compounds known as spherands, wherein the energetic price of assuming the binding conformation and desolvating the binding site is paid during the synthesis procedure rather than during complexation. Figure 16 shows the chemical structures of **48**–**56** which were used to illustrate this principle. Compound **54** contains six *m*-linked anisyl units whose OCH_3 groups are displayed alternately above and below the plane of the macrocycle. X-ray crystallography established that the O lone pairs of **54** are pointing into the fully desolvated roughly spherical central cavity (Figure 17a). X-ray crystal structures were also obtained for the **54**·Li^+ and **54**·Na^+ complexes. The hole diameters of **54,** **54**·Li^+ and **54**·Na^+ are 1.62, 1.48, and 1.73 Å, respectively, which indicates that the host **54** undergoes only very minor structural changes during complexation. In combination, these results establish that **54** is fully preorganized for cation binding.

What are the consequences of this preorganization toward binding strength? To answer this question, Cram and coworkers prepared compounds **49**–**53** which increase the number of *m*-anisyl units from 1 to 5 in a stepwise fashion relative to 18-crown-6 derivative **48**. Table 1 shows the values of ΔG° (kcal mol^{-1}) measured for these hosts toward the alkali-metal cations and NH_4^+ in $CDCl_3$ saturated with water by the picrate extraction method. Several trends are noteworthy: (i) Introduction of one or two anisyl units (**49** and **50**) lowers the overall binding affinity and selectivity toward the series of guests due to decreased preorganization relative to crown ether **48**; (ii) For compounds with three, four, or five anisyl units (**51**–**53**), which substantially define the spherand cavity, the affinity and selectivity for the smaller Na^+ and Li^+ cations becomes more pronounced.

Table 1 Binding constants ($-\Delta G^\circ$, kcal mol^{-1}, $CDCl_3$ saturated with D_2O) measured by the picrate extraction method.[34,51–53]

	Li^+	Na^+	K^+	Rb^+	Cs^+	NH_4^+
48	6.3	8.4	11.4	9.9	8.5	10.1
49	5.5	6.4	8.5	7.5	6.9	7.6
50	6.5	8.7	9.8	8.6	7.8	7.9
51	7.2	12.2	11.7	10.5	9.0	9.8
52	7.2	13.5	10.7	8.4	7.1	8.7
53	12.8	14.4	10.4	7.9	6.7	8.7
54	>23	19.2	–[a]	–[a]	–[a]	–[a]
55	<6	<6	<6	<6	<6	–[a]
56	8.3	10.1	8.9	10.4	13.9	9.1

[a]Not measured.

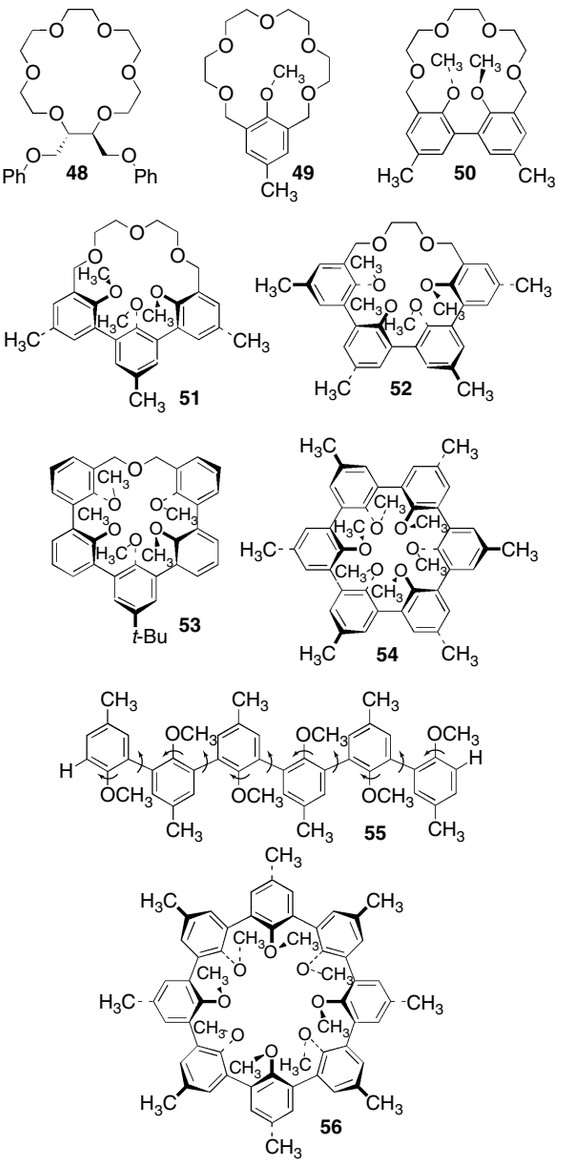

Figure 16 Chemical structures of selected hosts used by Cram to define the principle of preorganization.

For **54** with six anisyl units, the affinity for Li^+ increases by over 10 kcal mol^{-1} relative to **53** and the selectivity Li^+/Na^+ selectivity increases to >3.8 kcal mol^{-1}. Another interesting comparison concerns the relative complexing strength of **54** and **55**. Compounds **54** and **55** are related by the cleavage of one of the biaryl C–C bonds of **54** followed by addition of two H atoms; compound **55** can be viewed as an acyclic analog of **54**. Because compound **55** has a total of 11 C–C and C–O bonds that can undergo conformational changes, **55** has over 1000 conformations open to it. In order for **55** to complex cations, it would be necessary for **55** to assume a crescent conformation which would be

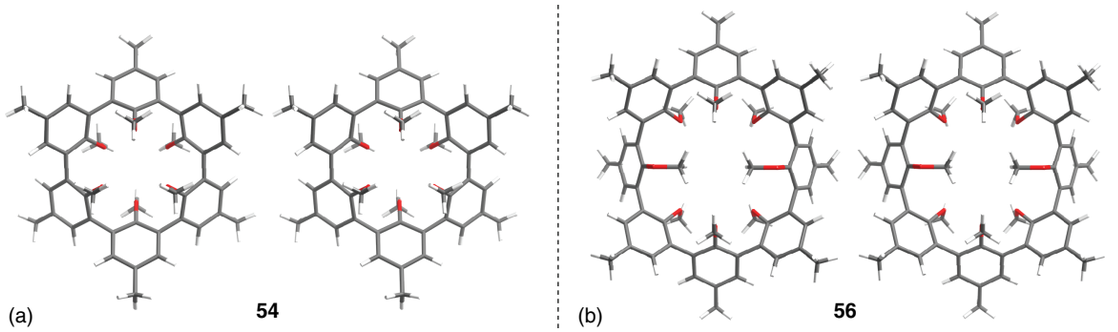

Figure 17 Stereoviews of the MMFF-minimized geometries of (a) **54** and (b) **56**. Color code: C, gray; H, white; O, red.

energetically very costly. Cram and coworkers were not able to detect any binding toward the various alkali cations by the picrate extraction method which allowed them to place an upper limit of $\Delta G^\circ < -6\,\text{kcal mol}^{-1}$. The cleavage of a single C–C bond in **54** to give **55** results in a decrease in affinity toward Li^+ of more than $17\,\text{kcal mol}^{-1}$! Such is the power of preorganization. Well-preorganized systems display high affinity and high selectivity in their complexation behavior.

Across the series of compounds given in Table 1, the highest affinity and highest selectivity are observed for host **54** that is complementary to the smallest alkali cation guests Li^+ and Na^+. Cram and coworkers also prepared host **56** which contains eight *m*-anisyl units and which accordingly possesses a larger cavity that is complementary to the larger cations (e.g., Cs^+). Table 1 shows that the affinities of **56** toward the alkali cations and NH_4^+ range from -8.3 to $-13.9\,\text{kcal mol}^{-1}$. Host **56** displays highest affinity for Cs^+, which is most complementary toward it, but the selectivities are not as high as those displayed by **54**. There are two main reasons for this difference. First, host **56** is not fully preorganized for binding Cs^+. This lack of preorganization is obvious in the X-ray crystal structure of free host **56** (Figure 17b) where two of the OCH_3 groups turn inward and thereby fill the cavity of **56**. Upon complexation with Cs^+, these OCH_3 group must turn outward, which is energetically costly. Second, host **56** is sizable enough to be able to complex the smaller cations (e.g., Li^+ and Na^+) as their partially solvated [e.g., $Li^+\cdot(H_2O)$ and $Na^+\cdot(H_2O)$] forms. These results highlight two of the reasons why it is so challenging to prepare hosts for larger guest species that are both preorganized and selective.

2.3.2 *Acyclic preorganization*

The most common approach toward preorganization of host molecules involves the formation of macrocycles in order to limit the conformational degrees of freedom available. It is also possible—although less common—to preorganize acyclic receptors by using other forms of conformational control. For example, Zimmermann and coworkers developed compound **57** which functions as a molecular tweezer (Figure 18).[54] Molecular tweezer **57** features two acridine π-surfaces held rigidly apart at a distance of $\approx$7 Å by a dibenz[*c*, *h*]acridine spacer. Compound **57** was found to complex to trinitrofluorenone (**58**) by $\pi-\pi$ interactions in $CDCl_3$ solution with $K_a = 172\,\text{M}^{-1}$. In contrast, control compounds that lack one of the acridine walls (**59**) or the rigid spacing unit (**60**) do not undergo complex formation

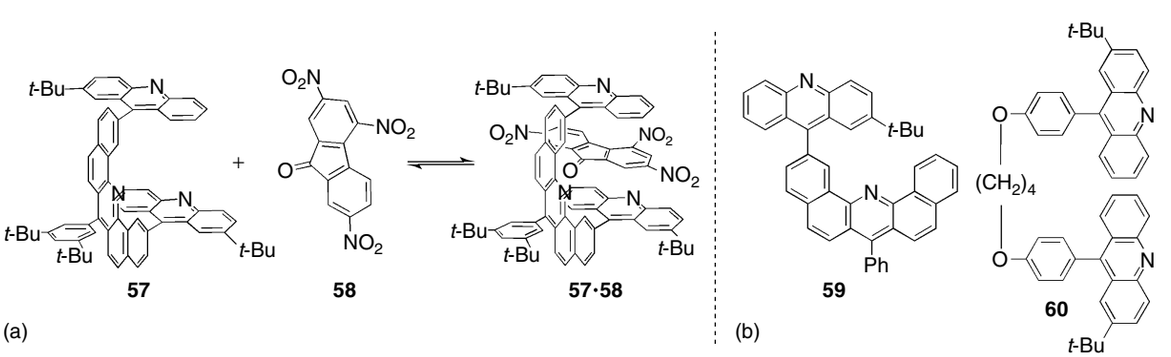

Figure 18 Molecular structures of (a) tweezer **57**, guest **58**, and the **57**·**58** complex, and (b) noncomplexing control compounds **59** and **60**.

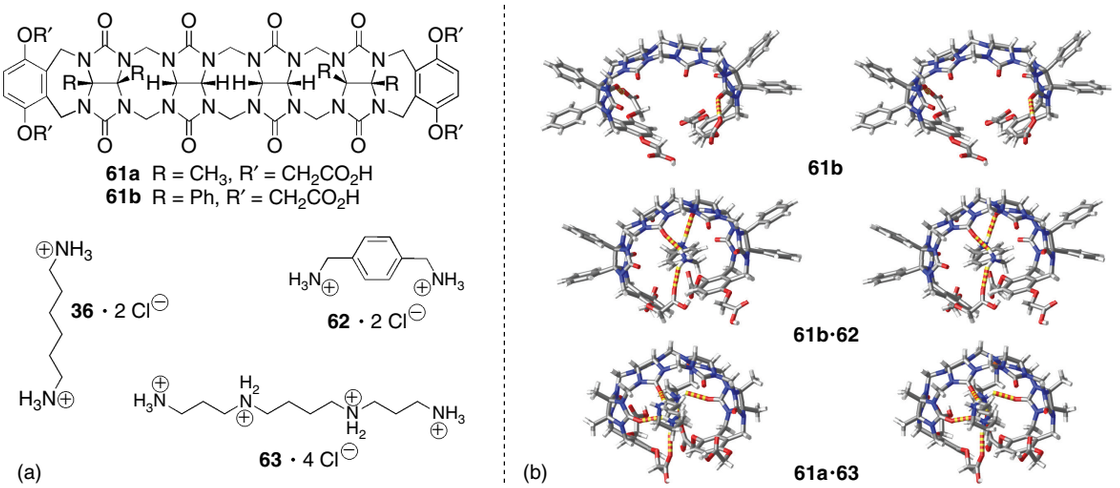

Figure 19 (a) Chemical structure of acyclic CB[*n*] congener **61** and three guests (**36, 62**, and **63**) and (b) X-ray crystal structures of **61b, 61b·62**, and **61a·63**. Color code: C, gray; H, white; O, red; H-bonds, red-yellow striped.

($K_a < 5\,M^{-1}$). One advantage of such acyclic receptors relative to their macrocyclic counterparts—by virtue of their lack of "walls"—is that the size and topology of the guest are not limited by volume of the molecular cavity.

As part of our interest in the CB[*n*] family of molecular containers and related compounds, we have decided to prepare acyclic CB[*n*] congener **61**.[55] Compound **61** is composed of four glycoluril units connected by pairs of CH_2 groups that are capped by carboxylic acid-substituted *o*-xylylene rings (Figure 19). All the substituents on the glycoluril rings (e.g., CH_3 and H) of **61a** are located on the same side of the molecule and point out of the cavity. Acyclic CB[*n*] congener **61** is relatively preorganized by design: (i) the fused five-membered rings of the glycoluril building blocks are relatively rigid, (ii) the eight-membered rings are conformationally restricted because of potential 1,5-diaxial interactions, and (iii) the seven-membered rings that connect the capping *o*-xylylene rings to the glycoluril oligomer are known to prefer the anticonformation[56,57] which further defines the cavity of **61**. Figure 19 shows the X-ray crystal structure of **61b** in its uncomplexed state. As expected, based on the considerations described above, **61** assumes a C-shaped geometry that defines a cavity. Compound **61** is soluble in water and displays a high affinity toward alkanediammonium ions. Most interesting for the present discussion is the comparable affinities of the **61a·36** ($K_a = 1.6 \times 10^8\,M^{-1}$) and CB[6]·**36** ($K_a = 2.9 \times 10^8\,M^{-1}$) complexes, which establishes that **61a** is as potent a receptor as the highly preorganized CB[6]. Interestingly, **61a** is a much less selective receptor than CB[6] because the acyclic nature of **61a** allows it to expand the size of its cavity to accommodate larger guests. Figure 19 also shows the X-ray crystal structures of the **61b·62** and **61a·63** complexes, which illustrate that **61** does not undergo substantial changes upon complexation.

2.3.3 *Desolvation*

One of the key aspects of Cram's definition of preorganization is that to achieve maximum binding affinity the binding sites of the host and guest should be poorly solvated before complexation. Since the degree of solvation of a host (guest) depends on the structure of both the host (guest) and the solvent, the extent of preorganization must also be regarded as solvent dependent. Consider, for example, Meijer's ureidopyrimidinone **64** which undergoes tight dimerization in $CHCl_3$ ($K_a > 10^6\,M^{-1}$) solution driven by the formation of four H-bonds (Figure 20).[58] This dimeric assembly falls apart when the solvent is switched to the more polar solvent $(CH_3)_2SO$ which is a much more strongly competitive hydrogen-bonding solvent. Conversely, when the hydrophobic effect is the major driving force for complexation, a change from aqueous solution to polar organic solvents may reduce binding affinity. For example, Smithrud and Diederich studied the strength of the complex between macrobicyclic receptor **65** and pyrene **66** in 18 different solvents that span the full range of polarity (e.g., CS_2 to H_2O).[59] They found that the $-\Delta G^\circ$ value for the complex decreased linearly as a function of $E_T(30)$ from 9.4 kcal mol^{-1} in H_2O : DMSO (dimethyl sulfoxide) (99 : 1) to 1.3 kcal mol^{-1} in CS_2. This large change in free energy of binding is attributed to solvation effects. The authors conclude that water is particularly favorable for apolar complexation because "water has the highest cohesive interactions and

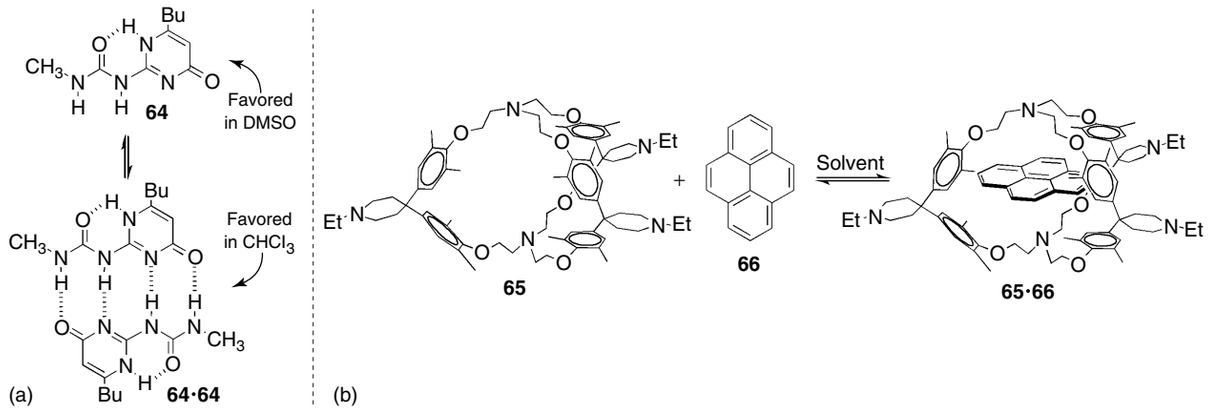

Figure 20 (a) Dimerization of **64** and (b) formation of the **65·66** complex.

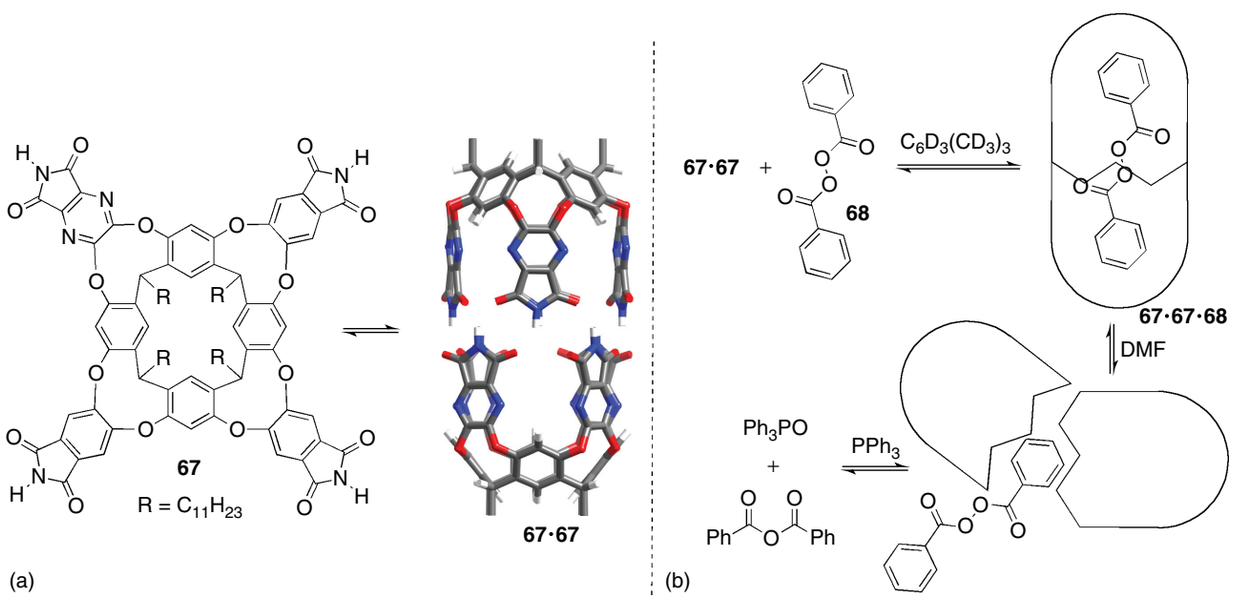

Figure 21 (a) Structure of resorcinarene **67** and its H-bonded dimer (**67·67**) and (b) complexation of benzoyl peroxide inside **67·67** which turns off its reactivity toward Ph_3P but can be restored by a H-bonding competitor like DMF which causes dissociation of the **67·67·68** capsular complex.

possesses by far the lowest molecular polarizability. *Both effects taken together* make it the best solvent for apolar complexation."[59]

A particularly interesting situation where (de)solvation plays an important role comes from the work of Rebek.[60–63] Rebek and coworkers prepared resorcinarene derivative **67** which features four imide functional groups (Figure 21). In its vase-like conformation, the four imide functional groups form a self-complementary array of H-bonding groups which can, in theory and in practice, result in the formation of a dimeric cylindrical capsule. Proton NMR spectra recorded for **67** in $CDCl_3$, CD_2Cl_2, C_6D_6, or $C_6D_5CD_3$ show a single set of resonances that are consistent with C_{4v} symmetry and the resonances for the imide NH groups appear downfield of a monomeric control compound, which strongly suggested the formation of dimeric capsule **67·67**. Subsequent studies established that the capsule **67·67** is filled with three solvating $CHCl_3$ molecules in this solvent.[61,62] Quite interestingly, when **67** is mixed with rigorously purified deuterated mesitylene $C_6D_3(CD_3)_3$—the largest commercially available deuterated solvent—**67** aggregates to form undefined materials which are poorly soluble.[63] Rebek and coworkers present the intriguing explanation that deuterated mesitylene $C_6D_3(CD_3)_3$ is simply too large to solvate the interior of the cavity of **67·67**. Since Nature abhors a vacuum, **67** assembles to form undefined (presumably better solvated) aggregates instead of dimeric capsule **67·67**. Compound

67 can be viewed as being preorganized to form dimeric capsule **67·67** in $CDCl_3$ but not in $C_6D_3(CD_3)_3$. Consequently, the use of deuterated mesitylene $C_6D_3(CD_3)_3$ as a solvent allowed them to study the complexation of suitable guests in the absence of competition from solvent filling the cavity of **67·67**. Because the size and shape of benzoyl peroxide are complementary to the cavity of **67·67**, the **67·67·68** complex is readily formed. Although **68** decomposes within 3 h at 70 °C in $C_6D_3(CD_3)_3$, the **67·67·68** complex survives for at least three days unchanged indicating a remarkable stabilization inside the capsule. Benzoyl peroxide **68** is so stable that it does not perform its usual oxidation of Ph_3P to Ph_3PO when encapsulated inside **67·67**. Quite interestingly, the normal reactivity of **68** can be "turned on" by the addition of competitive guests that better solvate the internal cavity of **67·67** and release free **68** or by the addition of the H-bond competitive solvent $HCON(CH_3)_2$ [DMF (dimethylformamide)] which hydrogen-bonds to the rim of monomeric **67** and thereby destabilizes the capsule releasing free reactive **68**. As described above, all these examples are readily understandable on the basis of the principle of preorganization as formulated by Cram. The take-home message is that, in designing strong noncovalent complexes, it is critical to consider the ground state structures of the solvated forms of the host, guest, and host·guest complex since the differences in free energy between the solvated forms determine the ΔG of complexation.

2.4 A related concept—predisposition

In the context of their studies of dynamic covalent chemistry, Sanders and coworkers introduced the concept of *predisposition*.[64] Sanders and coworkers studied the thermodynamically controlled macrocyclization of cinchonidine hydroxyester **69** and xanthene hydroxyester **70** (Figure 22). Remarkably, they found that **69** exclusively forms the cyclic trimer **71**, whereas **70** exclusively forms the cyclic dimer **72**. Mixtures of **69** and **70** undergo self-sorting to yield exclusively **71** and **72**. Quite interestingly, the conformational preferences of the monomer **69** are different from those of the cyclic trimer **71** as evidenced by changes in the coupling constants (**69**, $^3J_{H8-H9} = 3.8$ Hz; **71**, $^3J_{H8-H9} = 10.5$ Hz). This means that **69** is not preorganized to form **71** but rather that **69** is predisposed to form **71**. Sanders and coworkers state: "Predisposition, . . . should be thought of as a strong conformational or structural preference expressed by the building block once incorporated into a larger structure. . . . Conceptually, this idea is similar to the idea that certain amino acid residues in a peptide are helix-forming or zipper-inducing: these properties are not necessarily reflected in the conformational preferences of free amino acids in solution."[64]

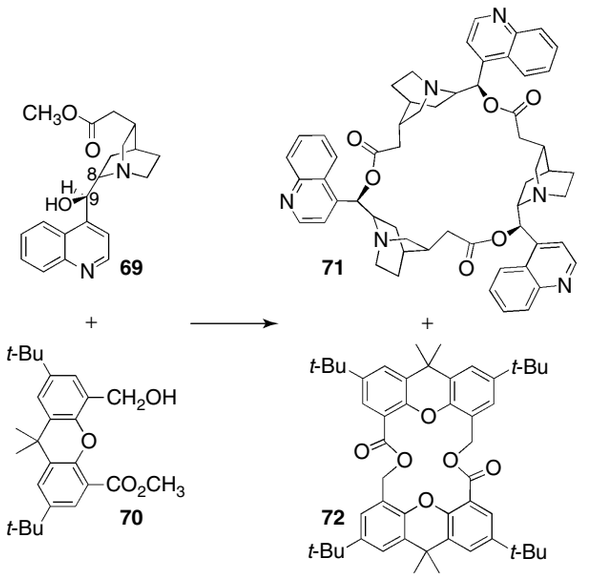

Figure 22 Thermodynamically controlled transesterification of a mixture of **69** and **70** giving only homotrimer **71** and homodimer **72** to the exclusion of heteromeric cycles.

2.5 Beyond the principle of preorganization

The examples presented throughout this chapter make it clear that the principles of complementarity and preorganization have played a defining role in the development of the foundations of supramolecular chemistry. Indeed, these basic principles also play a key role in the thought processes that guide contemporary supramolecular chemistry. However, because highly preorganized and highly selective receptors are typically structurally rigid and therefore generally unresponsive to environmental stimuli, they are less well suited for many application areas.

One current theme in supramolecular chemistry is the development of chemical sensing systems that operate in homogeneous solutions or under heterogeneous conditions. Contemporary chemical sensors need to quantify multiple analytes within a complex mixture. Although a one-host-one-analyte approach to analyze such mixtures is possible in theory, in practice the preparation of high-affinity and high-selectivity hosts for each analyte of interest would be prohibitively expensive and time consuming. Accordingly, a number of researchers have taken the approach employed by the human sensory system (e.g., tongue or nose) which relies on an array of receptors that bind to a variety of species with differential affinity and selectivity profiles.[5,65] The collective output of such a sensor array can be analyzed by statistical methods to yield the identities and concentrations of the components of the mixture (see **Uses of Differential Sensing and Arrays in Chemical Analysis**, Volume 2). For example, the Anslyn group has used

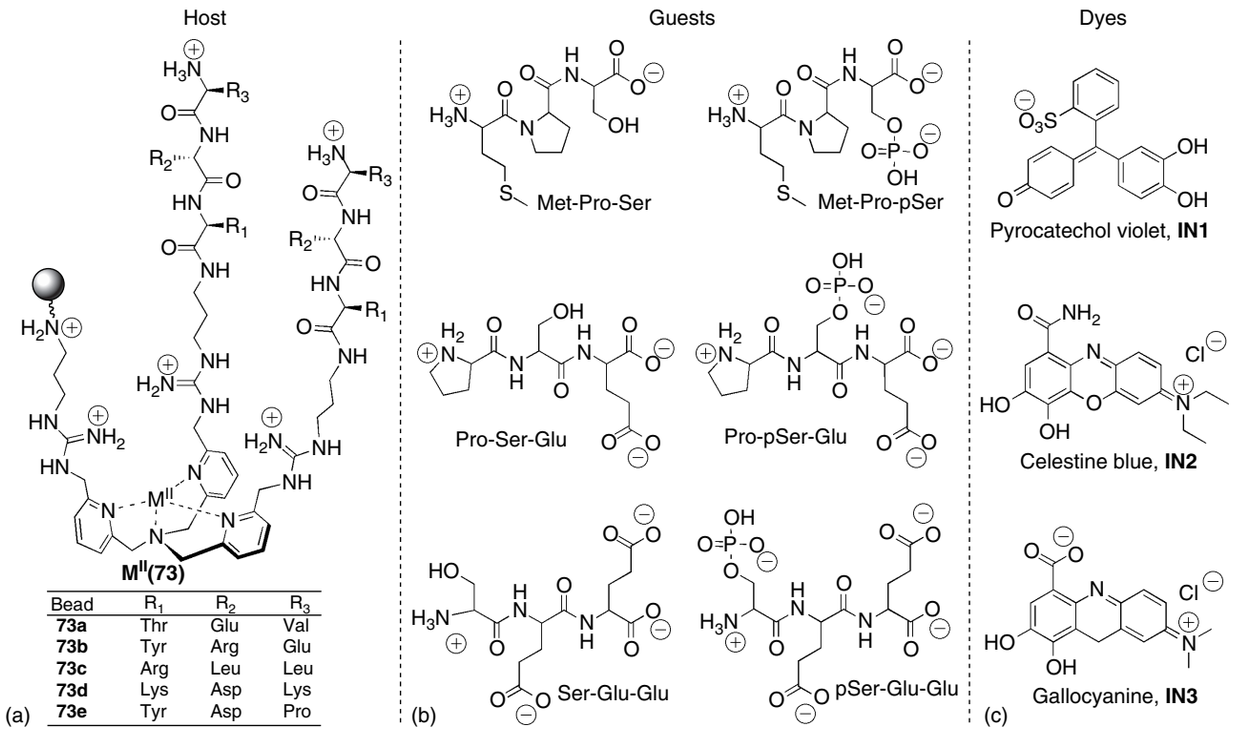

Bead	R_1	R_2	R_3
73a	Thr	Glu	Val
73b	Tyr	Arg	Glu
73c	Arg	Leu	Leu
73d	Lys	Asp	Lys
73e	Tyr	Asp	Pro

Figure 23 Structures of (a) resin-bound receptors **73a**–**73e**, (b) (phosphorylated) peptide guests, and (c) dyes employed in the indicator displacement assays.

indicator displacement assays[66] in combination with differential (i.e., cross-reactive) sensor arrays to pattern peptide phosphorylation of three model peptides (Figure 23).[67] To create a receptor that would exhibit differential response to these peptides and their phosphorylated analogs, a library of 6859 tripodal tripyridyl ligands (**73**) were synthesized on amine-functionalized tentagel resin. Initial screening of this library of receptors took place with the CuII·**73** complex with celestine blue (**IN1**) as indicator using Pro-pSer-Glu as analyte. The beads that showed significant indicator displacement were selected and sequenced, and five of them were resynthesized (**73a**–**e**) for use in the differential sensor array conducted in a 96-well plate format. All 90 combinations of **73a**–**e**, metal ion (Co(II), Ni(II), Cu(II)), indicator (**IN1**–**IN3**), and each tripeptide and its phosphorylated analog were arrayed in the 96-well plate and the UV–vis spectra were collected. Linear discriminant analysis was then used to differentiate between the six different (phosphorylated) peptides with nearly 90% confidence. This study highlights that arrays of hosts that lack lock-and-key type preorganization and selectivity but instead exhibit broader profiles of affinity and selectivity can be used advantageously to construct differential sensing arrays for fingerprinting of a variety of chemically and biologically important species.

A second research area of current interest where the principle of complementarity is used to discover molecules with interesting structures and functions is dynamic combinatorial chemistry (DCC).[68] For example, Sanders, Otto, and coworkers have studied the templated macrocyclization of (±)-**74** at pH 9.0 in water under aerobic conditions (see **Template Strategies in Self-Assembly**, Volume 5). In the absence of an ammonium ion template, a mixture of diastereomers of the various-sized macrocycles (e.g., *rac*-**75**–*rac*-**77**) is obtained (Figure 24). Remarkably, in the presence of $(CH_3)_4N^+I^-$ as a template, HPLC (high-performance liquid chromatography) analysis indicated the 400-fold amplification of a compound that was identified as *meso*-**75**. Given the potentially spacious cavity of *meso*-**75,** which is apparent from a consideration of its line bond and CPK structures shown in Figure 24, it was surprising that $(CH_3)_4N^+$ had such a large templating effect. Isothermal titration calorimetry (ITC) was used to determine the binding constant for the *meso*-**75**·$(CH_3)_4N^+$ complex ($K_a = 4 \times 10^6\,M^{-1}$) in 10 mM pH 9 borate buffer. To gain a better understanding of the geometry of this complex, ^{1}H NMR and CPK molecular modeling were performed. The ^{1}H NMR spectrum of *meso*-**75** alone is broad and featureless, which suggests that a large number of conformations are open to *meso*-**75**, that *meso*-**75** undergoes aggregation, or that a combination of both factors

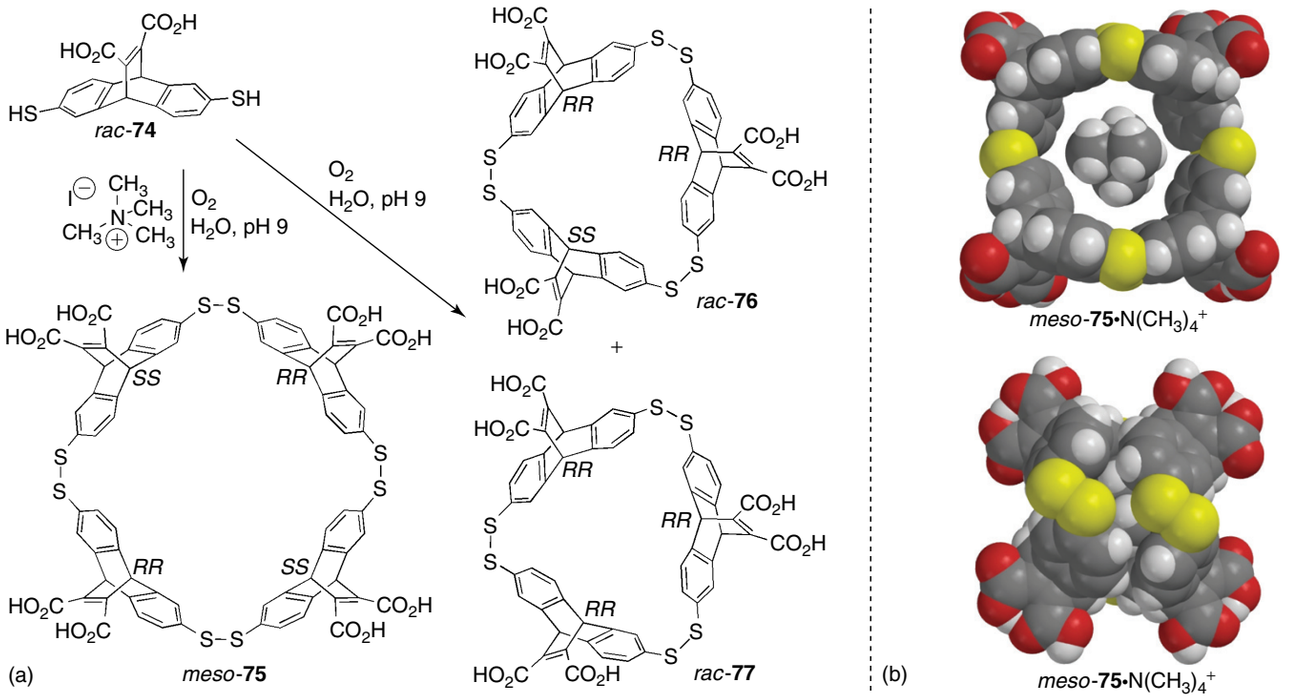

Figure 24 (a) Preparation of a dynamic combinatorial library of macrocycles in the presence or absence of $(CH_3)_4NI$ as template, and CPK model of the **75**·$N(CH_3)_4^+$ complex in (b) hypothetical open and (c) folded conformations.

is at play. Remarkably, in the presence of $N(CH_3)_4I$, the ^1H NMR exhibits a single set of sharp resonances, which is consistent with a single well-defined conformation for the *meso*-**75**·$N(CH_3)_4$ complex. Figure 24 shows molecular models for a hypothetical "open" conformation of *meso*-**75**·$(CH_3)_4N^+$ and for a "folded" conformation of *meso*-**75**·$(CH_3)_4N^+$ in which the $(CH_3)_4N^+$ cation is buried in the middle of the complex by cation–π interactions. This is a rare example of a nonnatural induced fit receptor in water. It is unlikely that *meso*-**75** would have been designed by applying the principles of complementarity and preorganization. However, through the judicious selection of building blocks with known affinity toward ammonium cations[36] and employing DCC, it is possible to discover anomalous and unexpected host–guest architectures. Some of these new hosts even behave in a biomimetic fashion forming complexes by an induced fit mechanism.

3 CONCLUSION

The field of supramolecular chemistry has developed at such a rapid pace since the pioneering work of Cram, Lehn, and Pedersen four decades ago that the core ideas of supramolecular chemistry now permeate to adjacent basic and applied scientific fields. In this chapter, we have described and illustrated by way of classical and contemporary examples two of the most important core ideas—namely the principle of complementarity and the principle of preorganization. To reiterate, the *principle of complementarity* states that "to complex, hosts must have binding sites which can simultaneously contact and attract the binding sites of the guests without generating internal strains or strong nonbonded repulsions." Examples of complementarity based on interactions between arrays of H-bond donors and acceptors, large π-surfaces, ions, and dipoles, or quadrupoles, and quadrupoles and quadrupoles were highlighted which form the foundation for the design of more complex systems that deploy multiple noncovalent interactions simultaneously. We have further seen how chiral host platforms are more complementary to one enantiomer of a racemic guest and how this enantioselectivity was used to devise an amino acid resolving machine. The clever design of the C_2-symmetric host used in this study by Cram and coworkers can be seen to presage the development of the wide variety of C_2-symmetric ligand systems currently employed in enantioselective catalysis.

Complementarity is necessary but not sufficient to ensure a high-affinity interaction between host and guest. For this purpose, Cram formulated *the principle of preorganization* which states that "the more highly hosts and guests are organized for binding and low solvation prior

to their complexation, the more stable will be their complexes." This principle manifests itself in numerous ways. For example, Zimmerman's complementary ureidodeazapterin **19**—which exists in two self-complementary dimeric forms via DDAA H-bonding arrays—is complementary to diamidonaphthyridine **24** via its ADDA tautomeric form. However, **22** or **23** cannot be considered preorganized for binding with **24** because energy must be spent to break up the homodimers **19·19**–**21·21** and then populate the **22** and **23** protomeric form. The spherands of Cram spectacularly illustrate the power of conformational preorganization. For example, although **54** and **55** differ only by two H-atoms, **54** binds Li^+ over 10^{12}-fold more tightly than **55**. This dramatic difference in affinity is due to the high enthalpic and entropic costs associated with **54** assuming the crescent geometry required to bind Li^+. Solvation also exhibits a dramatic effect on the degree of preorganization. A prime example comes from the work of Diederich, who showed that the value of $-\Delta G^\circ$ for the **65·66** complex is linearly related to the $E_T(30)$ value of the solvent. The principles of complementarity and preorganization operate in concert to determine which host–guest complexes form, their values of K_a, and ultimately the selectivity between competing complexes.

Although the principles of complementarity and preorganization have played major roles in the development of supramolecular chemistry as a discipline, there are a number of contemporary research topics in which strict adherence to the principle of preorganization may, in fact, prove detrimental. For example, in DCC, building blocks are selected that are expected to have a general complementarity to the template guest and the system as a whole responds minimizing the overall free energy of the system. A beautiful example from the groups of Sanders and Otto (Figure 24) showed that such approaches can generate hosts that operate by an induced fit mechanism that is more typically observed in biological systems. Another example where high preorganization can be detrimental is in the preparation of sensor arrays. In such sensor arrays, the use of hosts with good affinity and moderate selectivity, in combination with advanced statistical methods, allows the sensing of a broader range of analytes than would be possible with a single-host-single-analyte (e.g., lock-and-key) strategy. In other situations—such as the sequestration of toxic heavy metals from a complex mixture—the use of highly preorganized systems is still clearly warranted. Overall, the principles of complementarity and preorganization have supported the development of the field of supramolecular chemistry for four decades and will continue to do so for the foreseeable future.

ACKNOWLEDGMENTS

We thank the National Science Foundation (CHE-0615049 and CHE-0914745) for financial support.

REFERENCES

1. D. J. Cram and J. M. Cram, *Container Molecules and their Guests*, The Royal Society of Chemistry, Cambridge, 1994.
2. C. J. Pedersen, *Angew. Chem. Int. Ed. Engl.*, 1988, **27**, 1021–1027.
3. J. M. Lehn, *Angew. Chem. Int. Ed. Engl.*, 1988, **27**, 89–112.
4. D. J. Cram, *Angew. Chem. Int. Ed. Engl.*, 1988, **27**, 1009–1020.
5. A. T. Wright and E. V. Anslyn, *Chem. Soc. Rev.*, 2006, **35**, 14–28.
6. B. E. Collins and E. V. Anslyn, *Chem.—Eur. J.*, 2007, **13**, 4700–4708.
7. E. R. Kay, D. A. Leigh, and F. Zerbetto, *Angew. Chem. Int. Ed.*, 2007, **46**, 72–191.
8. J. F. Stoddart, *Chem. Soc. Rev.*, 2009, **38**, 1802–1820.
9. K. Mueller, C. Faeh, and F. Diederich, *Science*, 2007, **317**, 1881–1886.
10. F. Hof and F. Diederich, *Chem. Commun.*, 2004, 477–480.
11. E. Fisher, *Ber.*, 1894, **27**, 2985–2993.
12. D. E. Koshland Jr., *Proc. Natl. Acad. Sci. U.S.A.*, 1958, **44**, 98–104.
13. R. Taylor and O. Kennard, *Acc. Chem. Res.*, 1984, **17**, 320–326.
14. C. B. Aakeroy and K. R. Seddon, *Chem. Soc. Rev.*, 1993, **22**, 397–407.
15. J. R. Fredericks and A. D. Hamilton, *Comprehensive Supramolecular Chemistry*, Pergamon, Oxford, 1996, vol. 9, pp. 565–594.
16. M. M. Conn and J. Rebek Jr., *Chem. Rev.*, 1997, **97**, 1647–1668.
17. L. Brunsveld, B. J. B. Folmer, E. W. Meijer, and R. P. Sijbesma, *Chem. Rev.*, 2001, **101**, 4071–4097.
18. L. J. Prins, D. N. Reinhoudt, and P. Timmerman, *Angew. Chem. Int. Ed.*, 2001, **40**, 2382–2426.
19. G. R. Desiraju, *Acc. Chem. Res.*, 2002, **35**, 565–573.
20. G. R. Desiraju, *Chem. Commun.*, 2005, 2995–3001.
21. L. Stryer, *Biochemistry*, W.H. Freeman, New York, 1995.
22. Y. Kyogoku, R. C. Lord, and A. Rich, *Proc. Natl. Acad. Sci. U.S.A.*, 1967, **57**, 250–257.
23. Y. Kyogoku, R. C. Lord, and A. Rich, *Biochim. Biophys. Acta*, 1969, **179**, 10–17.
24. W. L. Jorgensen and J. Pranata, *J. Am. Chem. Soc.*, 1990, **112**, 2008–2010.
25. T. J. Murray and S. C. Zimmerman, *J. Am. Chem. Soc.*, 1992, **114**, 4010–4011.

26. D. A. Bell and E. V. Anslyn, *Tetrahedron*, 1995, **51**, 7161–7172.
27. H.-B. Wang, B. P. Mudraboyina, J. Li, and J. A. Wisner, *Chem. Commun.*, 2010, **46**, 7343–7345.
28. B. A. Blight, A. Camara-Campos, S. Djurdjevic, *et al*. *J. Am. Chem. Soc.*, 2009, **131**, 14116–14122.
29. J. Granja and M. Ghadiri, *J. Am. Chem. Soc.*, 1994, **116**, 10785–10786.
30. P. S. Corbin and S. C. Zimmerman, *J. Am. Chem. Soc.*, 1998, **120**, 9710–9711.
31. S. Ghosh and L. Isaacs, *J. Am. Chem. Soc.*, 2010, **132**, 4445–4454.
32. N. S. Isaacs, *Physical Organic Chemistry*, Longman Group, Essex, 1995.
33. C. J. Pedersen, *J. Am. Chem. Soc.*, 1967, **89**, 7017–7036.
34. D. J. Cram and K. N. Trueblood, *Top. Curr. Chem.*, 1981, **98**, 43–106.
35. H.-J. Buschmann, *Chem. Ber.*, 1985, **118**, 2746–2756.
36. P. C. Kearney, L. S. Mizoue, R. A. Kumpf, *et al*. *J. Am. Chem. Soc.*, 1993, **115**, 9907–9919.
37. D. A. Dougherty, *Science*, 1996, **271**, 163–168.
38. J. H. Williams, *Acc. Chem. Res.*, 1993, **26**, 593–598.
39. G. W. Coates, A. R. Dunn, L. M. Henling, *et al*. *Angew. Chem. Int. Ed. Engl.*, 1997, **36**, 248–251.
40. J. Lagona, P. Mukhopadhyay, S. Chakrabarti, and L. Isaacs, *Angew. Chem. Int. Ed.*, 2005, **44**, 4844–4870.
41. J. W. Lee, S. Samal, N. Selvapalam, *et al*. *Acc. Chem. Res.*, 2003, **36**, 621–630.
42. S. Liu, C. Ruspic, P. Mukhopadhyay, *et al*. *J. Am. Chem. Soc.*, 2005, **127**, 15959–15967.
43. C. Márquez, R. Hudgins, and W. Nau, *J. Am. Chem. Soc.*, 2004, **126**, 5806–5816.
44. D. J. Cram, H.-J. Choi, J. A. Bryant, and C. B. Knobler, *J. Am. Chem. Soc.*, 1992, **114**, 7748–7765.
45. K. N. Houk, A. G. Leach, S. P. Kim, and X. Zhang, *Angew. Chem. Int. Ed.*, 2003, **42**, 4872–4897.
46. E. B. Kyba, K. Koga, L. R. Sousa, *et al*. *J. Am. Chem. Soc.*, 1973, **95**, 2692–2693.
47. M. Newcomb, J. L. Toner, R. C. Helgeson, and D. J. Cram, *J. Am. Chem. Soc.*, 1979, **101**, 4941–4947.
48. A. P. Davis, D. N. Sheppard, and B. D. Smith, *Chem. Soc. Rev.*, 2007, **36**, 348–357.
49. R. F. Ludlow and S. Otto, *Chem. Soc. Rev.*, 2008, **37**, 101–108.
50. N. Sakai, J. Mareda, and S. Matile, *Acc. Chem. Res.*, 2008, **41**, 1354–1365.
51. R. C. Helgeson, B. J. Selle, I. Goldberg, *et al*. *J. Am. Chem. Soc.*, 1993, **115**, 11506–11511.
52. D. J. Cram and G. M. Lein, *J. Am. Chem. Soc.*, 1985, **107**, 3657–3668.
53. S. P. Artz and D. J. Cram, *J. Am. Chem. Soc.*, 1984, **106**, 2160–2171.
54. S. C. Zimmerman and C. M. VanZyl, *J. Am. Chem. Soc.*, 1987, **109**, 7894–7896.
55. D. Ma, P. Y. Zavalij, and L. Isaacs, *J. Org. Chem.*, 2010, **75**, 4786–4795.
56. R. P. Sijbesma and R. J. M. Nolte, *J. Am. Chem. Soc.*, 1991, **113**, 6695–6696.
57. R. P. Sijbesma, S. S. Wijmenga, and R. J. M. Nolte, *J. Am. Chem. Soc.*, 1992, **114**, 9807–9813.
58. F. H. Beijer, R. P. Sijbesma, H. Kooijman, *et al*. *J. Am. Chem. Soc.*, 1998, **120**, 6761–6769.
59. D. B. Smithrud and F. Diederich, *J. Am. Chem. Soc.*, 1990, **112**, 339–343.
60. S. K. Körner, F. C. Tucci, D. M. Rudkevich, *et al*. *Chem.—Eur. J.*, 2000, **6**, 187–195.
61. A. Shivanyuk and J. Rebek, *J. Am. Chem. Soc.*, 2002, **124**, 12074–12075.
62. A. Shivanyuk and J. Rebek, *Angew. Chem. Int. Ed.*, 2003, **42**, 684–686.
63. A. Scarso, L. Trembleau, and J. Rebek, *J. Am. Chem. Soc.*, 2004, **126**, 13512–13518.
64. S. J. Rowan, D. G. Hamilton, P. A. Brady, and J. K. M. Sanders, *J. Am. Chem. Soc.*, 1997, **119**, 2578–2579.
65. C. N. LaFratta and D. R. Walt, *Chem. Rev.*, 2008, **108**, 614–637.
66. S. L. Wiskur, H. Ait-Haddou, J. J. Lavigne, and E. V. Anslyn, *Acc. Chem. Res.*, 2001, **34**, 963–972.
67. T. Zhang, N. Y. Edwards, M. Bonizzoni, and E. V. Anslyn, *J. Am. Chem. Soc.*, 2009, **131**, 11976–11984.
68. P. T. Corbett, J. Leclaire, L. Vial, *et al*. *Chem. Rev.*, 2006, **106**, 3652–3711.